IL NUOVO CIMENTO Vol. 34 C, N. 1 Gennaio-Febbraio 2011
DOI 10.1393/ncc/i2011-10816-y

Colloquia: IFA2010

Study of atmospheric aerosol by means of nuclear techniques with accelerator at LABEC

G. Calzolai

Dipartimento di Fisica e Astronomia, Università di Firenze and INFN, Sezione di Firenze Firenze, Italy

(ricevuto il 30 Luglio 2010; approvato il 10 Settembre 2010; pubblicato online l'1 Marzo 2011)

Summary. — The atmospheric aerosols, despite their tiny concentration in the air, have a relevant impact on a wide range of issues, spanning from the local to the global scale. Many epidemiologic studies on human exposures to ambient particulate matter have clearly established a statistically significant correlation between fine-particles concentration in the air and health effects. Moreover, increasing interest originates by the role of aerosols in climate change, and in particular in global warming and changes in hydrological cycles. Nuclear techniques have been demonstrated to be an effective tool for aerosol study. In particular, the IBA (Ion Beam Analysis) techniques may allow the detection of all the elements present in the aerosol samples. Radiocarbon measurements, performed by AMS (Accelerator Mass Spectrometry), can give fundamental information about the sources of the aerosol carbonaceous fraction. Without claiming to be exhaustive, a brief description of the role of these techniques in the aerosol study is given in the present paper, with a special attention to their applications at the INFN-LABEC laboratory of Florence.

PACS 89.60.-k – Environmental studies.
PACS 82.80.Ej – X-ray, Mössbauer, and other γ-ray spectroscopic analysis methods.
PACS 92.60.Mt – Particles and aerosols.
PACS 93.85.Np – Radioactivity methods.

1. – Aerosol properties and effects

As is well known, atmosphere is not only composed of gases: it also contains suspended particles both solid and liquid, characterised by sizes spanning over about 5 orders of magnitude, from $\sim 1\,\mathrm{nm}$ up to $\sim 100\,\mu\mathrm{m}$. The suspension of solid and liquid particles in a gas is called *aerosol*. The suspended particles (*airborne particulate matter*) may be directly introduced into the air by natural or anthropogenic sources (primary aerosol), or produced in air by chemical-physical reactions of gases, vapours or suspended particles (secondary aerosol). Their concentrations in air may range from hundreds of $\mathrm{ng/m^3}$ in remote areas up to hundreds of $\mu\mathrm{g/m^3}$ in the most polluted industrial or urban areas,

depending on many parameters (*e.g.*, emission sources and meteorological conditions) [1]. Despite their tiny concentrations, atmospheric aerosols have a relevant impact on both human health (respiratory and cardio-respiratory problems linked to air pollution [2]) and on the environment (visibility, atmospheric radiative transfer [3]). The role of atmospheric aerosol in producing the aforementioned effects is determined by aerosol basic (and often interdependent) properties such as chemical composition, water solubility, optical properties, atmospheric residence time and size distribution (in mass, volume, number or surface).

Health effects are clearly connected to the different penetration of the particles into the breathing apparatus, with smaller particles more easily reaching the deeper levels and therefore being potentially more dangerous. Nowadays, a statistically relevant correlation between particulate matter levels and adverse impacts on human health has been established, and reduced lung function, lung cancer, cardiopulmonary mortalities and elevated rates of premature mortality have been associated to short-term and/or long-term exposures to fine particulate matter [2].

Among the environmental effects, the reduction of visibility [4], due to the scattering and absorption of sunlight by atmospheric particles, is the most commonly experienced effect. Moreover, as aerosols carry most of the toxic metals, acids and nitrates of the atmosphere, dry or wet aerosol deposition may produce soil and water contamination and damages to vegetation and monuments [5].

Nowadays, great concern is aroused by the interaction of aerosols with the Earth's climate: in fact, aerosols contribute to the Earth's radiation budget by both direct and indirect mechanisms. As direct effects, aerosols scatter and absorb both sunlight and thermal radiation, which is also emitted by the same aerosols. As an indirect effect, aerosols act as cloud condensation nuclei (CCN) and ice nuclei (IN), inducing cloud and fog formation and modifying microphysical cloud properties. As far as the indirect effects are concerned, it is worth stressing that clouds have a large role in the Earth's radiation budget, as they cover about 60% of the surface of our planet. There is evidence that small changes in macrophysical and microphysical properties (*e.g.*, coverage and droplet size) significantly affect climate. The enhancement of the reflection of solar radiation due to the more abundant but smaller cloud droplets in a cloud (cloud albedo or Twomey effect) and the increase of cloud lifetime (and thus of its reflectivity) due to the reduced precipitation efficiency in clouds having smaller droplets (cloud lifetime or second indirect effect) are among the indirect effects having larger impact on the Earth's radiation budget [6, 7].

2. – Basics on aerosol sampling and determination of the emission sources

In an aerosol sampler, the air is pumped through the same sampler and particles are collected by *impaction* and/or *filtration*. In the impaction process the air stream is forced to make an abrupt change in direction: the heavier particles, due to their higher inertia, cannot follow the air stream and impact onto a surface (impaction foil). In the filtration process, the air stream is forced (by a pressure gap application) to pass through a filter (or membrane) whose fibres intercept the particles.

Particles are generally conveniently classified on the bases of their aerodynamic diameter (D_{ae}), which is defined as the size of a unit-density sphere with the same aerodynamic characteristics [8]. Particles with $D_{\mathrm{ae}} < 10\,\mu$m and $D_{\mathrm{ae}} < 2.5\,\mu$m are referred as PM_{10} and $\mathrm{PM}_{2.5}$, respectively.

Aerosol samples are mostly collected on a daily basis by sequential particle samplers. In order to collect by filtration all the aerosol particles with dimensions lower than a fixed aerodynamic diameter (for example, PM_{10} or $PM_{2.5}$), a pre-impaction stage is installed upstream of the filter to eliminate the larger particles.

Continuous samplers may also be used to obtain a higher time resolution. For example, the *streaker* samplers allow the aerosol sampling with hourly resolution, in both the fine ($D_{ae} < 2.5\,\mu$m) and the coarse ($2.5\,\mu\text{m} < D_{ae} < 10\,\mu$m) fractions of particulate matter [9]. Briefly, in a streaker sampler, particles are separated on two different stages by a pre-impactor and an impactor. The pre-impactor removes particulate matter with aerodynamic diameter $D_{ae} > 10\,\mu$m. The aerosol coarse fraction impacts on a Kapton foil, while the fine fraction is collected on a Nuclepore filter. The two collecting plates (Kapton and Nuclepore) are paired on a cartridge, which rotates at constant speed for a week: this produces a circular continuous deposit of particular matter (the "*streak*") on both the stages.

Another kind of sampler is the multistage cascade impactor, in which the aerosol particles are collected on different impaction foils depending on their D_{ae} (*size-fractionated*, or *size-segregated*, samples). There are a certain number of different multicascade impactors, which differ for the number of stages and for the ranges of selectable D_{ae}. As an example, in Florence a SDI (Small Deposit area Impactor) sampler by Dekati [10] is avalaible. It is a 12-stages impactor, with the following cut-off D_{ae}: 8.57, 4.12, 2.70, 1.68, 1.07, 0.90, 0.60, 0.35, 0.23, 0.15, 0.09, 0.05 μm.

Since the characteristic aerosol temporal variations occur on several scales, from diurnal patterns (hours) through synoptic behaviour (days) to seasonal trends (months), the desired sampling *time resolution* can vary from hours to months. The collection of size-fractionated samples with a high time resolution (of the order of hours) is the best solution to get a detailed aerosol characterization and to study the physical-chemical processes involving aerosols (production, transformation, transport, removal). However, this would produce huge amounts of samples to be analysed and aerosol deposits collected by multimode samplers with good time resolution may be too small also for very sensitive analysis methods. As a consequence, when studying long-term behaviours it is convenient to sample with daily resolution. Sampling strategies (*i.e.* size and time resolution) have to be accurately chosen on the basis of the specific problem investigated (air quality monitoring, pollution source identification, climate studies, etc.).

Actually, the determination of the aerosol emission sources is a fundamental step for both the assessment of pollution abatement strategies and the study of climate change. The identification and the quantification of the contributions of the different emission sources are mainly obtained thanks to the application of statistical multivariate analysis such as receptor models (PCA, APCA, PMF, etc.), which require the knowledge of suitable markers for each emission source.

3. – IBA techniques for the study of atmospheric aerosols

Whatever the sampling strategy (even if fully optimised for the aim of the study), every sampling campaign produces large amounts of few μg particulate samples, which should be fully characterised: fast, quantitative, highly sensitive and multielemental (*i.e.* simultaneous for a wide range of atomic numbers) analytical methods are thus required. Non-destructiveness is also an important issue in order to extend the range of detectable elements by complementary techniques applied to the same sample. IBA (*Ion Beam Analysis*) techniques successfully cope with all these requirements. A further advantage of IBA is given by the fact that they do not need any pre-treatment of the sample, thus

minimising possible sample contaminations (in our specific application, the analysis is performed directly on the particles deposited on the filtering support). Finally, IBA techniques are mandatory for the analysis of *streaker* samples, since they allow a point-by-point analysis.

The most used IBA technique for the aerosol study is the PIXE (*Particle Induced X-ray Emission*) analysis: it is based on the analysis of the X-rays emitted by the sample after excitation, which is produced by the interaction with an accelerated particle (generally proton) beam. PIXE provides, in a few minutes measuring time, the concentrations of all the elements with atomic number $Z > 10$. Among these elements there are markers of specific components or sources of particulate matter such as marine aerosol (Na, Cl), mineral dust (Al, Si, Ca, Ti, Sr), sulphates (S), biomass burning products or biogenic emissions (K, Zn, Rb), heavy oil combustion (V, Ni), incinerator emissions (K, Zn, Pb), traffic and industrial emissions (Mn, Ni, Cu, Zn, Pb).

The complementary use of other IBA techniques such as PESA (*Particle Elastic Scattering Analysis*), for the determination of H, C, N, O, and PIGE (*Particle Induced Gamma-ray Emission*), for the analysis of other low-Z elements (such as Li, B, F, Na, Al), allows the detection of all the elements present in the aerosol samples and, thus, a complete mass closure. PESA and PIGE are based on the detection of scattered beam particles and γ-rays, respectively, which are produced by the interaction of a beam of accelerated charged particles with the nuclei in the sample (target).

Due to the self-absorption effect of the X-rays of lower energy inside the single aerosol particles, PIXE may underestimate the concentrations of the lighter elements, such as Na, Mg and Al. Therefore, a further advantage of the simultaneous application of PIXE and PIGE (apart from the detection of elements invisible to PIXE, like F) is the possibility of determining experimentally the self-absorption correction factors, in order to provide correct concentrations of the lighter elements detectable by PIXE [11].

Finally, elemental concentrations in air are deduced from the elemental concentrations measured in the sample through the knowledge of the sampling parameters (area of the deposit, air flow rate, duration of sampling).

3˙1. *Experimental.* – At the LABEC laboratory an external beam facility is fully dedicated to PIXE/PIGE measurements of elemental composition of atmospheric aerosols. On this line, the proton beam is extracted in air through a 7.5 μm thick Upilex window and the aerosol samples are positioned at a distance of about 1 cm from the window, perpendicular to the beam. The volume of atmosphere between the bombarded sample and the X-ray detectors is saturated with helium, to reduce the absorption of the emitted radiation. The beam size is set by a collimator (usually to $1.0 \times 2.0\,\mathrm{mm}^2$) located in the last section of the in-vacuum beam line. A Faraday Cup positioned just behind the sample allows the measurement of the integrated beam current. Two X-ray detectors optimised for low and medium-high X-ray energies, respectively, are used in order to obtain an efficient simultaneous detection of all the elements (X-ray production cross sections range over 3 orders of magnitude). The first one is a Silicon Drift Detector (SDD), the latter is a Si(Li) detector (145 eV and 175 eV FWHM energy resolution at the 5.9 keV Mn K_α line, respectively).

Finally, γ-rays for PIGE analysis are detected by a 60 mm $\times$23 mm Ge detector, with 28% efficiency and 1 keV FWHM energy resolution at 1.33 MeV.

More details on the PIXE-PIGE set-up may be found in [12].

Two different set-ups, the "daily and size-segregated sample set-up" and the "streaker sample set-up", allow an easy handling, positioning, changing and scanning of samples

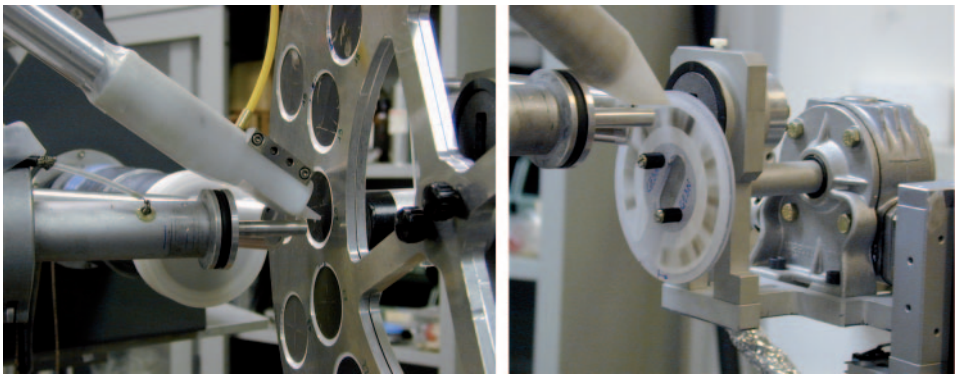

Fig. 1. – Pictures of the experimental set-up for external PIXE-PIGE analysis on daily/size-segregated samples (on the left) and streaker samples (on the right).

collected by sequential samplers or multistage cascade impactors and streaker samplers, respectively (fig. 1). Both the scanning of the aerosol filters and the change of the samples are automatically controlled by the acquisition system.

During irradiation of daily samples (about 5–10 min per sample), the filters are moved in front of the beam so that most of the area of deposit is analysed, in order to average over possible sample inhomogeneities.

Size-segregated samples are absolutely inhomogeneous; therefore, the analysis is performed by scanning with a homogeneous beam an area of known dimensions ($\sim 1\,\mathrm{cm}^2$), larger than the whole deposit. The analysis of every single multicascade impactor stage takes about 10–15 min.

The streak produced by the streaker sampler is analysed "point by point" using a beam spot (1 mm × 2 mm) that corresponds to one hour of aerosol sampling. One "point" is irradiated for about 3–5 min, so that scanning the whole streak requires about 9–15 hours.

At LABEC, PESA is performed in an in-vacuum chamber with two fully depleted Si p-n diode detectors arranged at 30° and 150° scattering angles, in order to detect, respectively, H and N, O and C. The detector placed at forward angle is strongly collimated to compensate the higher elastic scattering cross section; the solid angle subtended by the forward and backward detectors are 0.2 msr and 4.3 msr, respectively.

For all the detected elements, elemental thicknesses ($\mu\mathrm{g/cm}^2$) are obtained by comparing the sample yields with a sensitivity curve measured in the same geometry on a set of reference standards of known elemental composition.

Detection limits are about $10\,\mathrm{ng/m}^3$ for low-Z elements (Na, Mg, Al, Si, P, S, Cl, K, Ca, Ti, V, Cr) and about 1–2 $\mathrm{ng/m}^3$, or below, for medium-high–Z elements (Mn, Fe, Ni, Cu, Zn, As, Se, Br, Sr, Zr, Pb). The detection limits for PESA are about 0.02, 1.0, 0.5, 0.5 $\mu\mathrm{g/m}^3$ for H, C, N and O, respectively.

The uncertainty of the elemental concentrations is determined by a sum of independent uncertainties on standard sample thickness (5%), sampling parameters ($\sim$ 5%, depending on the sampler), and counting statistics (5–10% for H and C; 10–30% for N; 10–20% for O; 2–20% or higher when concentrations approach the detection limits for $Z > 10$).

3˙2. *Examples of applications of IBA measurements*

Daily samples: Saharan Dust Intrusions. Daily PM_{10} levels are currently monitored by local Environmental Agencies. The EU Air Quality Directives set some limits about many air quality parameters. Without going into the details, the 2008/50/EC directive sets an annual average PM_{10} concentration limit of $40\,\mu g/m^3$ and a daily PM_{10} concentration limit of $50\,\mu g/m^3$ that has not to be exceeded more than 35 days per year. The directive also states that possible natural contributions, leading to concentrations exceeding the aforementioned limits, may be subtracted. In this perspective, it is important noting that, in Southern Europe, the desert dust transported from North Africa gives a relevant contribution to the aerosol concentrations. The identification of Saharan dust intrusions is therefore mandatory in order to correctly apply the directive.

PIXE analysis is very powerful in the assessment of the contributions from these episodes due to its outstanding capability in detecting all the soil-related elements. As an example, a Saharan dust intrusion was identified during a sampling campaign conducted in Montelupo Fiorentino (a little town about 20 km west of Florence) in 2002 [13]. As shown in fig. 2, PM_{10} concentrations rapidly raised up, reaching a maximum value of $75\,\mu g/m^3$, together with soil-related elements (such as Si and Al) concentrations. The soil dust contribution, calculated as the sum of the principle oxides of the soil-related elements, was assessed to be about 40%, and therefore it was fundamental for the PM_{10} standard exceedance. Backward trajectory calculations performed with the HYSPLIT transport model (by NOAA Air Resource Laboratory) confirmed the hypothesis of a Saharan dust intrusion episode, as shown in fig. 3.

The study of desert dust transports is very important also for the research on climate. IBA techniques have been effectively used for these studies. As examples, they have been applied for the study of the variations of the aerosol properties during air mass transports from North Africa [14, 15], and of the desert dust composition [16, 17]. IBA techniques have also been applied for the study of mineral dust in Antarctica for paleoclimatic investigations [18, 19].

Hourly samples: the traffic source. As aforementioned, the measurement of suitable markers for each emission source is mandatory for the application of receptor models for the aerosol source apportionment. Samplings with hourly resolution are very helpful in this task, mainly to assess the contribution of industrial and traffic sources, which are characterised by rapidly variations in the aerosol emissions. Up to 2001, elements such as Br and, mainly, Pb were very effective markers for the traffic, but, as is well known, in 2001 leaded gasoline was banned: new markers for this source were needed. Presently, in areas not affected by specific industrial emissions, good markers for such source are Cu and Zn, emitted by the consumption of vehicular mechanical parts. Figure 4 reports some results on streaker samples collected in the same urban traffic sampling site (in Florence), respectively before and after 2001. As can be seen, in both cases these markers have similar patterns, confirming the hypothesis of a common source. Moreover, their concentrations also rise during the rush hours, while decreasing during the nights and the week-ends, when traffic also decreases [20].

Actually, Cu and Zn may be emitted in other processes than the traffic-related ones (as an example, they can be produced by industrial activities such as metalwork). Therefore, the use of these elements as markers of the traffic in order to perform source apportionment on daily samples should be supported by evidences obtained by hourly samplings.

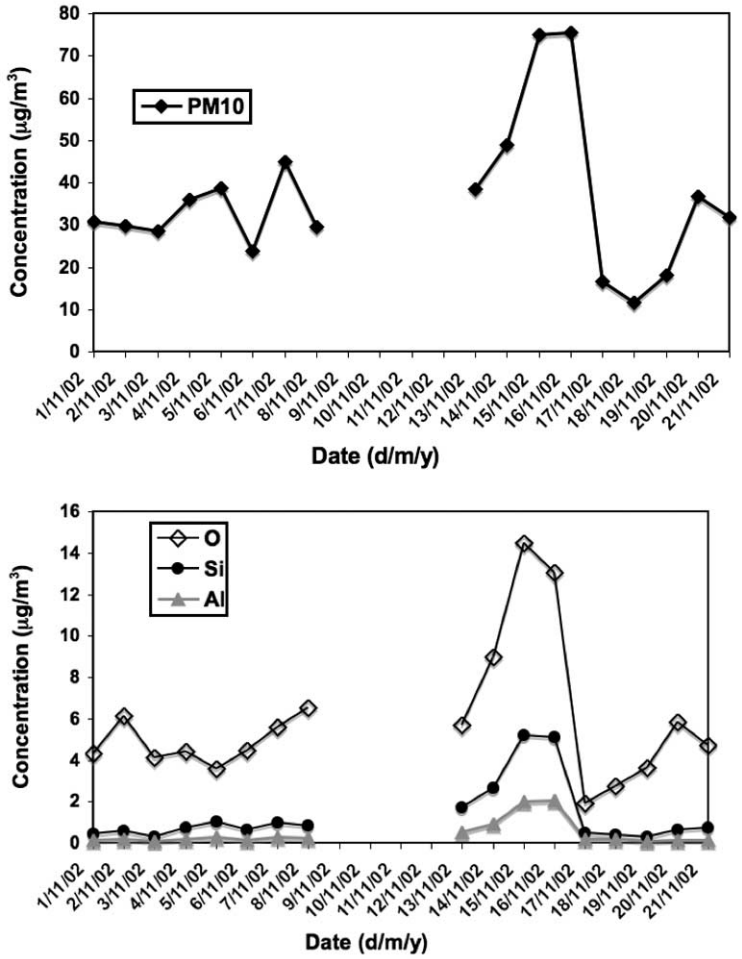

Fig. 2. – Concentrations of PM_{10} (upper panel) and soil-related elements (Si and Al; lower panel) during a Saharian dust intrusion event (days 14–16/11/2002) and during the days immediately before and after it. In the lower panel the O concentration is also shown: it also increases, since the soil-related elements are present in the mineral dust as oxides.

Moreover, samplings with hourly resolution are fundamental to assess the contributions of the industrial sources, since industrial emissions may vary very rapidly depending on the working phases (examples may be found in [21, 22]).

Size-segregated samples: examples of dimensional distributions. As aforementioned, the aerosol effects on human health are clearly connected to the particles dimensions, since the smaller the particles the deeper they can go into the respiratory system. Some elements are more harmful than others, since they are known as toxic, or even carcinogenic. Therefore, the knowledge of the dimensional distributions of the aerosol and of the related elemental compositions is a very important issue. Aerosol samplings with a multistage cascade impactor allow the determination of such profiles. Aerosols produced by natural sources or by mechanical processes are generally larger than the aerosol particles

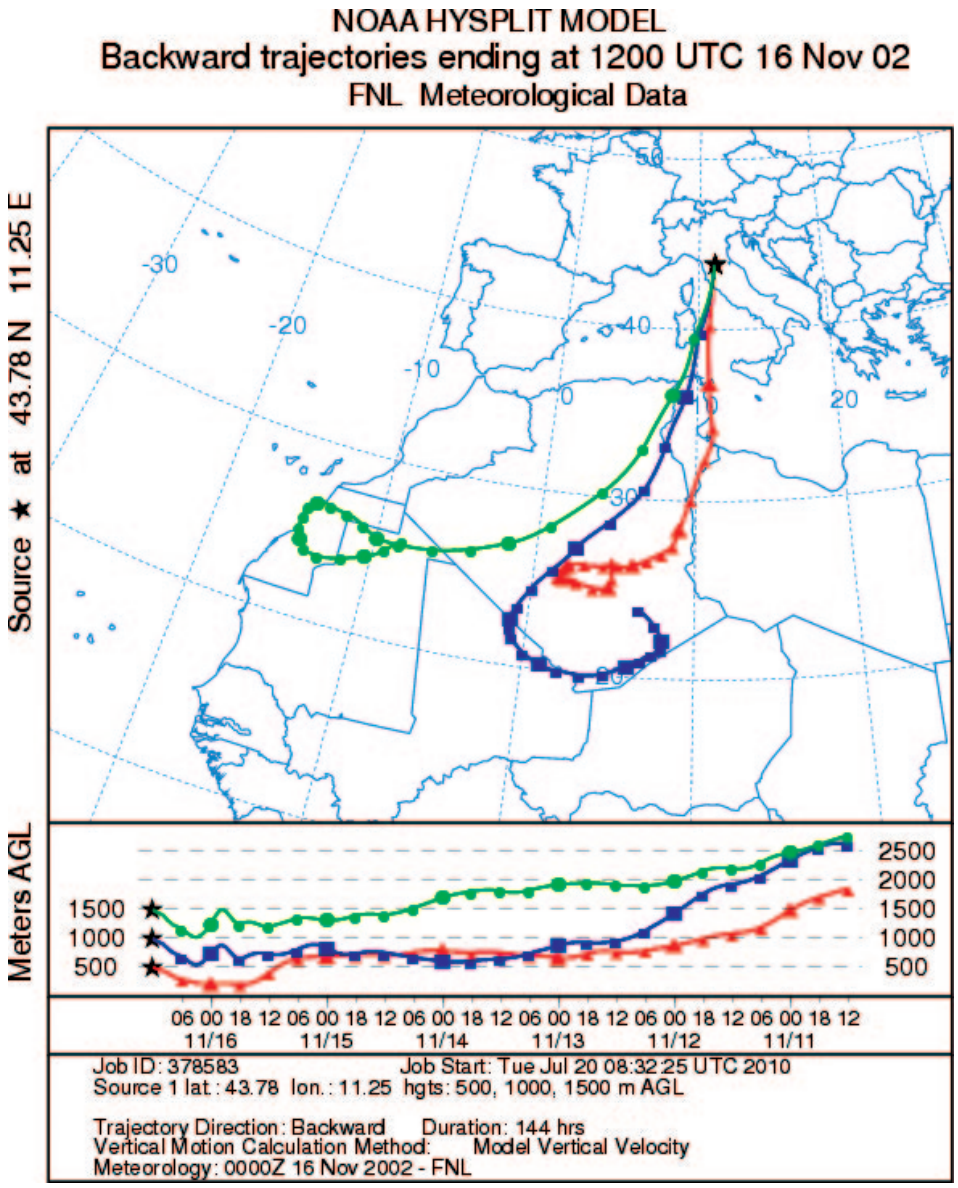

Fig. 3. – Backward trajectories calculated with the HYSPLIT model: air masses reaching the sampling site on 16/11/2002 came from the desert areas of Northern Africa.

produced by combustion processes. In fig. 5, some examples of dimensional distributions for Si, S and K are reported, as they can be measured by analysing the samples collected by a SDI multicascade impactor. Si is primarily present in the coarse particles, since it is mostly present in soil dust. S is an element mainly related to combustion processes and thus is more abundant in the fine aerosol fraction. K has a bi-modal distribution: the coarse particles are due to natural sources, while the fine particles are generated in combustion processes.

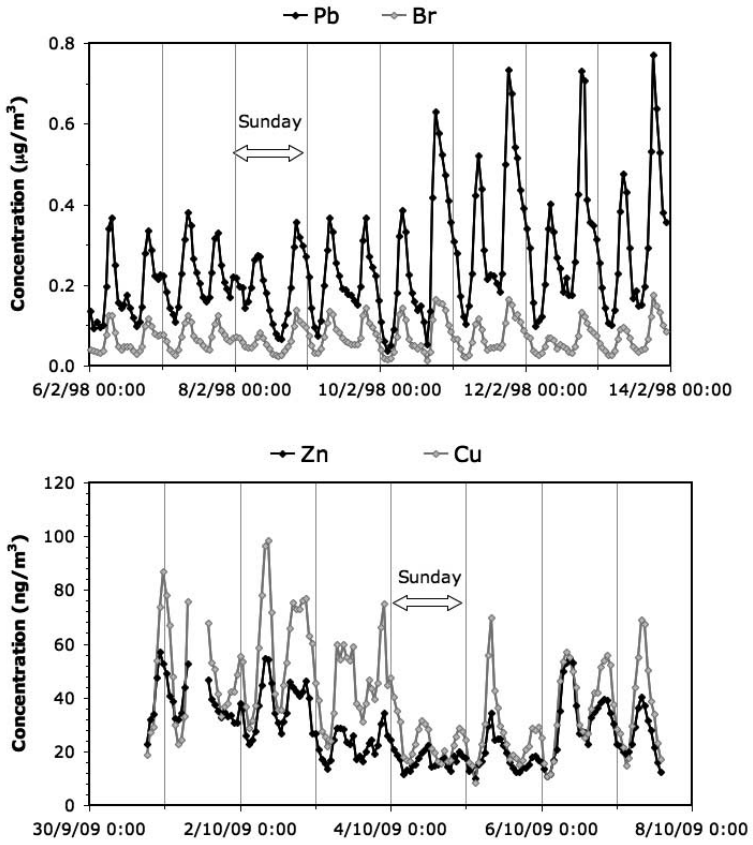

Fig. 4. – Concentrations of traffic source markers (Pb and Br before 2001 and Cu and Zn after 2001, when leaded fuel was banned) during two sampling weeks in an urban traffic sampling site.

4. – Radiocarbon AMS measurements for the study of the aerosol carbonaceous fraction

4˙1. *The aerosol carbonaceous fraction.* – Carbon is typically the largest elemental fraction of atmospheric aerosol particles, present in many different chemical and physical forms. This extreme diversity is at the origin of the recently increased interest in carbonaceous aerosols as it leads to important effects on both human health and climate modification. Carbonaceous particles can constitute about 40% of urban aerosol, and can be also more abundant depending on the location and on the particle size fraction [23].

The total carbon (TC) present as aerosol in the atmosphere can be expressed as the sum of organic carbon (OC) and elemental carbon (EC).

EC has a graphitic microstructure, and is emitted as primary particles (soot) from incomplete combustion processes possibly occurring when either fossil fuel or biomass are burnt (therefore, EC is mainly anthropogenic). Primary OC particles can be emitted from combustion sources, together with EC, or from natural sources such as debris, pollen, spores and algae. OC can also be formed in the atmosphere as secondary aerosol through gas-phase photochemical processes [24].

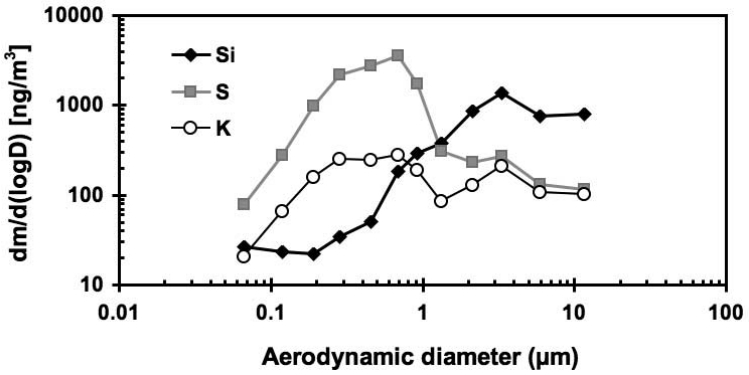

Fig. 5. – Examples of dimensional distributions of Si, S and K.

EC, the main constituent of soot, is almost exclusively responsible for the light absorption of the aerosols. Because of this property, EC is often referred to as black carbon (BC). OC is formed by hundreds of different organic compounds; concerning its optical properties, OC is mainly light scattering, since only two classes of organic compounds (polycyclic aromatics hydrocarbons and humic-like substances) are slightly light absorbing [23, 24]. Due to these different optical properties, EC and OC alter the radiative properties of the atmosphere in opposite ways, and thus play an opposite role in the aerosol radiative forcing.

4˙2. *Radiocarbon measurements of the aerosol carbonaceous fraction.* – Among the three natural isotopes of carbon, only ^{14}C is unstable and it is thus called "radiocarbon": it decays via β emission to ^{14}N with a half-life of 5730 years. Radiocarbon is mainly produced in the stratosphere and in the troposphere by nuclear reaction of thermal neutrons on atmospheric ^{14}N, according to the reaction $^{14}\mathrm{N(n,p)}^{14}\mathrm{C}$. After oxidation to CO_2, it spreads into the atmosphere, into the oceans and into the biosphere, through the plant photosynthesis and the food chain. Thanks to these processes living organisms have approximately the same radiocarbon concentration as the atmosphere; when the organism dies, it ceases to exchange CO_2 with the atmosphere and it behaves like a closed system, with its radiocarbon concentration decreasing according to the radioactive decay. By this way, fossil fuels (such as charcoal, gasoline and diesel) and the aerosol produced by their combustion are in optimum approximation ^{14}C-free, while the aerosol particles produced by biogenic sources are characterised by a similar concentration to the present atmosphere. On these bases, radiocarbon is a powerful tool for distinguishing aerosol sources, due to its unique power to discriminate fossil (*i.e.* ^{14}C-free) from contemporary carbon, *i.e.* to discriminate between carbon from anthropogenic fossil fuel combustion and biomass components [25].

By international convention, the radiocarbon concentration of a sample is usually expressed relative to the one present in the reference year 1950, as fraction of modern carbon (f_m) [26]:

$$f_\mathrm{m} = \frac{(^{14}\mathrm{C}/^{12}\mathrm{C})_\mathrm{sample}}{(^{14}\mathrm{C}/^{12}\mathrm{C})_\mathrm{AD1950}}\,.$$

As a consequence, fossil materials are characterised by a null fraction of modern carbon ($f_\mathrm{m,fossil} = 0$), while the fraction of modern carbon of the contemporary sources of aerosol

($f_{\mathrm{m,bio}}$) can be evaluated from time series of $^{14}CO_2$ [27]. In fact, during the 1950s and 1960s the atmospheric radiocarbon concentrations raised up due to the nuclear tests and they have been decreasing since the atmospheric nuclear test ban.

On the bases of a simple two-source model, the contributions of the fossil and contemporary sources to the carbonaceous fraction of interest in the sample can easily be obtained by the following relations [25]:

$$C_{\mathrm{tot}} \cdot f_{\mathrm{m}}(\mathrm{C}) = C_{\mathrm{fossil}} \cdot f_{\mathrm{m,fossil}} + C_{\mathrm{bio}} \cdot f_{\mathrm{m,bio}},$$
$$C_{\mathrm{tot}} = C_{\mathrm{fossil}} + C_{\mathrm{bio}},$$

where $f_{\mathrm{m}}(\mathrm{C})$ is the measured fraction of modern carbon in the carbonaceous fraction C, present in the sample with a concentration C_{tot}, while C_{fossil} and C_{bio} are the concentrations of C originating from fossil and biomass sources, respectively.

This simple approach presents the main limitation that does not allow the discrimination between biomass burning and biogenic sources, as both these sources are characterised by a contemporary content of radiocarbon. A full disambiguation of the three carbonaceous sources (fossil, biogenic and wood burning) can be obtained when radiocarbon measurements are performed on the EC and OC separate fractions. In fact, the EC is produced only in combustion processes, *i.e.* it cannot derive from a biogenic source. Therefore, for the EC, the simple two-source model provides the contributions of all the possible sources, the fossil and the wood-burning ones (respectively $\mathrm{EC_{fossil}}$ and $\mathrm{EC_{wb}}$).

Concerning OC, the two-source model only allows the discrimination between the contributions from fossil ($\mathrm{OC_{fossil}}$) and non-fossil sources (biogenic, $\mathrm{OC_{bio}}$, and from wood burning, $\mathrm{OC_{wb}}$). The concentration of OC deriving from wood burning ($\mathrm{OC_{wb}}$) can be evaluated starting from $\mathrm{EC_{wb}}$ if the EC/OC emission ratio is known for the wood burning source, *i.e.* if $(\mathrm{EC/OC})_{\mathrm{ER,wb}}$ is independently estimated by measurements at the source or by literature data. By this way, $\mathrm{OC_{bio}}$ can be evaluated by subtracting $\mathrm{OC_{wb}}$ from the non-fossil carbon (taking into account for the different fractions of modern carbon between the biogenic source and the wood-burning one, since the burnt wood is generally about 30 years old) [28].

4˙3. *Experimental*. – Since 2004, the LABEC laboratory has been involved in AMS measurements for radiocarbon dating. The LABEC AMS system is described in [29]. In order to be analysed by AMS radiocarbon measurements, the samples have to be properly prepared; at LABEC, they have to be inserted into the ion source of the accelerator as graphite pellets. A sample preparation line dedicated to aerosol samples should allow the separation of EC and OC during the preparation of the graphite beads; this separation was not possible in the already running sample preparation line for radiocarbon dating.

A new sample preparation line designed to fulfil the EC/OC separation requirement has been recently installed at LABEC [30]. As a first step, it was tested for measurements of TC. The overall accuracy of both the sample preparation and the AMS measurements was tested, with good results, by preparing some samples from the reference material C7 provided by IAEA, with a certified radiocarbon content ($f_{\mathrm{m}} = 0.4953 \pm 0.0012$), comparable with the one expected for aerosol.

Preliminary tests on a few summer samples collected in an urban background sampling site in Milan indicated that the fossil source contribution to the TC was $\sim 50\%$ in the sampling days. These tests, although not significant for air quality studies because of the low number of analysed samples, are very encouraging since the results well agree with literature data [31]. Tests on the radiocarbon measurements on the separate EC and OC

fractions are in progress and specific sampling campaigns focused on the carbonaceous aerosol source apportionment are planned.

* * *

The author warmly acknowledges her colleagues, supervisors and mentors for their collaboration and support: Dr. S. Nava, Dr. M. Chiari, Dr. M. Fedi and Prof. F. Lucarelli from the University of Florence and INFN-Florence; Dr. V. Bernardoni, Dr. G. Valli and Dr. R. Vecchi from the University of Milan and INFN-Milan; Dr. E. Cuccia and Prof. P. Prati from the University of Genoa and INFN-Genoa.

REFERENCES

[1] Hinds W. C., *Aerosol Aerosol Technology – Properties, behavior, and measurement of airborne particles* (John Wiley & Sons) 1999.
[2] Pope C. A. III and Dockery D. W., *J. Air Waste Manag. Assoc.*, **56** (2006) 709.
[3] Forster P., Ramaswamy V., Artaxo P., Bernsten T., Betts R., Fahey D. W., Haywood J., Lean J., Lowe D. C., Myrhe G., Nganga J., Prinn R., Raga G., Schulz M. and Van Dorland R., *Changes in Atmospheric Constituents and in Radiative Forcing*, in: *Climate Change 2007: The Physical Science Basis. Contribution of Working Group I to the Fourth Assessment Report of the Intergovernmental Panel on Climate Change*, edited by Solomon S., Qin D., Manning M., Chen Z., Marquis M., Averyt K.B., Tignor M. and Miller H. L. (Cambridge University Press, Cambridge, UK, New York, USA) 2007.
[4] Watson J. G., *J. Air Waste Manag. Assoc.*, **52** (2002) 628.
[5] Sabbioni C., *Sci. Total Environ.*, **167** (1995) 49.
[6] Haywood J. and Boucher O., *Rev. Geophys.*, **38** (2000) 513.
[7] Lohmann U. and Feichter J., *Atmos. Chem. Phys.*, **5** (2005) 715.
[8] Marple V. A. and Willeke K., *Atmos. Environ.*, **10** (1976) 891.
[9] Formenti P., Prati P., Zucchiatti A., Lucarelli F. and Mandò P. A., *Nucl. Instrum. Methods B*, **113** (1996) 359.
[10] Maenhaut W., Hillamo R., Mäkelä T., Jaffrezo J. L., Bergin M. H. and Davidson C. I., *Nucl. Instrum. Methods B*, **109/110** (1996) 482.
[11] Calzolai G., Chiari M., Lucarelli F., Nava S. and Portarena S., *Nucl. Instrum. Methods B*, **268** (2010) 1540.
[12] Calzolai G., Chiari M., Garcia Orellana I., Lucarelli F., Migliori A., Nava S. and Taccetti F., *Nucl. Instrum. Methods B*, **249** (2006) 928.
[13] Chiari M., Lucarelli F., Mazzei F., Nava S., Paperetti L., Prati P., Valli G. and Vecchi R., *X-ray Spectrom.*, **34** (2005) 323.
[14] Marenco F., Bonasoni P., Calzolari F., Ceriani M., Chiari M., Cristofanelli P., D'Alessandro A., Fermo P., Lucarelli F., Mazzei F., Nava S., Piazzalunga A., Prati P., Valli G. and Vecchi R., *J. Geophys. Res.*, **111** (2006) D24202.
[15] Cristofanelli P., Marinoni A., Arduini J., Bonafé U., Calzolari F., Colombo T., Decesari S., Duchi R., Facchini M. C., Fierli F., Finessi E., Maione M., Chiari M., Calzolai G., Messina P., Orlandi E., Roccato F. and Bonasoni P., *Atmos. Chem. Phys.*, **9** (2009) 4603.
[16] Formenti P., Rajot J. L., Desboeufs K., Chevaillier S., Caquineau S., Nava S., Chiari M., Triquet S., Journet E., Gaudichet A., Alfaro S., Haywood J., Coe H. and Highwood E., *J. Geophys. Res.*, **113** (2008) D00C13.
[17] Formenti P., Nava S., Prati P., Chevaillier S., Klaver A., Lafon S., Mazzei F., Calzolai G. and Chiari M., *J. Geophys. Res.*, **115** (2010) D01203.
[18] Marino F., Castellano E., Nava S., Chiari M., Ruth U., Wegner A., Lucarelli F., Udisti R., Delmonte B. and Maggi V., *Geophys. Res. Lett.*, **36** (2009) L23703.

[19] Marino F., Calzolai G., Caporali S., Castellano E., Chiari M., Lucarelli F., Maggi V., Nava S., Sala M. and Udisti R., *Nucl. Instrum. Methods B*, **266** (2008) 2396.
[20] Del Carmine P., Lucarelli F., Mandò P. A., Valerio M., Prati P. and Zucchiatti A., *Nucl. Instrum. Methods B*, **150** (1999) 450.
[21] Chiari M., Del Carmine P., Garcia Orellana I., Lucarelli F., Nava S. and Paperetti L., *Nucl. Instrum. Methods B*, **249** (2006) 584.
[22] Mazzei F., D'Alessandro A., Lucarelli F., Marenco F., Nava S., Prati P., Valli G. and Vecchi R., *Nucl. Instrum. Methods B*, **249** (2006) 548.
[23] Pöschl U., *Angew. Chem. Int. Ed.*, **44** (2005) 7520.
[24] Watson J. G., Chow J. C. and Chen L.-W. A., *Aerosol Air Qual. Res.*, **5** (2005) 65.
[25] Currie L., *Radiocarbon*, **42** (2000) 115.
[26] Mook W. G., Van Der Plicht J., *Radiocarbon*, **41** (1999) 227.
[27] Levin I. and Kromer B., *Radiocarbon*, **39** (1997) 205.
[28] Szidat S., Jenk T. M., Synal H.-A., Kalberer M., Wacker L., Hajdas I., Kasper-Giebl A. and Baltensperger U., *J. Geophys. Res.*, **111** (2006) D07206.
[29] Fedi M. E., Cartocci A., Manetti M., Taccetti F. and Mandò P. A., *Nucl. Instrum. Methods B*, **259** (2007) 18.
[30] Calzolai G., Bernardoni V., Chiari M., Fedi M., Lucarelli F., Nava S., Riccobono F., Taccetti F., Valli G. and Vecchi R., *Nucl. Instrum. Methods B*, **269** (2011) 203.
[31] Lewis C. W., Klouda G. A. and Ellenson W. D., *Atmos. Environ.*, **38** (2004) 6053.